C. R. Chimie 22 (2019) 188–197

Contents lists available at ScienceDirect

Comptes Rendus Chimie

www.sciencedirect.com

Full paper/Mémoire

Elaboration and characterization of a low-cost porous ceramic support from natural Tunisian bentonite clay

Rania Chihi, Issam Blidi, Malika Trabelsi-Ayadi, Fadhila Ayari*

Laboratoire d'application de la chimie aux ressources et substances naturelles et à l'environnement (LACReSNE), Faculté des sciences de Bizerte, Zarzouna, Bizerte 7021, Tunisia

ARTICLE INFO

Article history:
Received 15 July 2018
Accepted 5 December 2018
Available online 14 January 2019

Keywords:
Bentonite
Ceramic support
Extrusion method
Sintering
Characterization

ABSTRACT

Ceramic supports from bentonite have become a hot research topic because of their low cost and abundance in many countries. This article describes the development and the characterization of a microfiltration support elaborated using an extrusion method followed by sintering at different temperatures (950, 1000, and 1100 °C). X-ray fluorescence, X-ray diffraction, Fourier transform infrared, scanning electron microscopy, transmission electron microscopy, and differential thermal analysis were used for the characterization of the raw material. The resulting support was characterized by scanning electron microscopy, mechanical and chemical resistance, and water permeability. Each tube was 150 mm in length, with an external diameter of 8 mm and an internal diameter of 5 mm.

1. Introduction

More then ever, the world demand for clear water, which requires better water treatment technology. According to the World Health Organization, 2.2 million people die of diarrhea-related disease every year most often caused by waterborne infections [1]. Membranes are recommended over other technologies for water treatment like distillation, disinfection, or media filtration. The use of organic membranes is more promoted; unfortunately, they are too expensive as economic applications in depollution control.

To treat great volumes of wastewater we need high fluxes and low costs. Ceramic membranes present, compared with polymeric membranes, enhanced mechanical, thermal, chemical stability, and long life time. Herein, we present a brief overview (see Table 1) of the advantages and disadvantages of ceramic membranes. Over the past decades, their applications have been fixed for small-scale industrial application, which is not suitable for polymeric membranes.

These inorganic membranes are suitable for a water purification process, such as oil–water separation, hazardous waste treatment, and industrial wastewater [3]. The commercial membrane technology is accessible for hardness, heavy metals, bacteria removal (microfiltration, MF), for virus and colloid removal (ultrafiltration, UF), and dissolved organic matter removal (nanofiltration), for desalination, and for ultrapure water production (reverse osmosis) [4,5]. Materials of this kind are the most suitable future challenging to produce an efficient, reliable, and selective separation with significant permeate flux for the treatment of considerable volumes of wastewater.

As recognized in the literature, many researches are target to produce less expensive ceramic membranes from abundant natural materials such as dolomite, pyrophyllite, apatite, fly ash, phosphate, pozzolan, clay mineral, and so forth. Uddin [6] described the production of tubular ceramic support from pyrophyllite clay via extrusion method for MF applications. Bouzerara et al [7] described the manufacturing of membrane support from doloma and kaolin mixtures proposed for MF and UF processes. Mamoudi et al [8] described the development of tubular porous support from natural apatite recommended for UF

* Corresponding author.
E-mail address: fadhilaayari@yahoo.fr (F. Ayari).

https://doi.org/10.1016/j.crci.2018.12.002
1631-0748/

Table 1
Advantages and disadvantages of ceramic membrane [2].

Advantages	Disadvantages
Able to resist high temperatures up to 280 °C. A special development onto modules and system could reach up to 700 °C	Brittle. Need a careful handling
Excellent corrosion resistance (toward organic solvent and a wide pH range)	
Suitable for cleaning and steam sterilization high mechanical strength	Most ceramic membranes are in disc or tubular shape; possess low surface Area/volume ratio
Able to endure in harsh condition, e.g., high acid or alkaline solution	
Possess long life time	The investment cost of ceramic membrane is very high
High membrane flux for porous membrane	

and MF applications. Saffaj et al [9–11] elaborated MF and UF membranes from natural Moroccan clay as a support and cordierite. Archiou et al [12] proposed a flat ceramic MF membrane elaborated from natural Moroccan pozzolan. Fang et al [13] manufactured a new ceramic membrane spherical fly ash for MF of rigid particle suspension and oil-in-water emulsion. Barrouk et al [14] developed ceramic membranes from natural and synthetic phosphate for the treatment of textile effluent. Sayehi et al [15] proposed the formation of a flat membrane from kaolin and potassium phosphate with appropriate elaboration parameters and the effect of their separation performance.

Clays, especially bentonite, have attracted much attention for numerous researches because of their high sorption properties, their high surface area, and high porosity [16,17]. The cost of these materials remains to be significantly low and they are abundant in many countries.

Our challenge is the elaboration of a low-cost support made of a natural and abundant new clay from Gabes, south of Tunisia. This region was discovered as a potential source of clay minerals. Several researchers addressed their investigation to develop supports of natural clay such as kaolin [18,19], cordierite [20], and zeolite [21].

The main objective of this study was the elaboration of tubular ceramic support by extrusion, using local bentonite as a starting material. The second part was to evaluate flexural mechanical strength, chemical resistance, and water permeability of our samples.

2. Materials and methods

2.1. Materials

2.1.1. Starting material

The raw material is bentonitic clay from Gabes (southern Tunisia). It was crushed for 20 min with the assistance of a motor crusher (Retsh, France), and then sieved to a fine powder with mesh size 100 μm.

2.1.2. Elaboration of porous support

The elaboration of tubular support was done in three stages: the first one is the preparation of paste mixed from powder clay with a plasticizer and binding additives in an aqueous solution, the second stage involves the extrusion of the sample, and the third one is based on the consolidation by thermal treatment of the obtained tube. The process used to produce tubular support is similar to that already described in detail in this previous work [29] to elaborate mineral support from Tunisian clay. The optimized formulation of the ceramic support contains (values are given in wt %) as follows:

- smectite clay: 84;
- plasticizer: amijel (Cplus 12076, Cerestar): 4;
- binder: methocel (Dow Chemical Company, France): 4;
- porosity agent: starch (RG 03408, Cerestar): 8.

The paste was synthesized from a mixture of raw bentonite powder and organic additive in an optimal formulation, and the mixture was homogenized with progressive addition of water. A block appeared at the end of this phase. After aging for 2 days, the paste was extruded with a screw speed of 0.02 m min^{-1}. Each tube obtained had 150 mm of length, an external diameter of 8 mm, and an internal diameter of 5 mm. The tubes were set on stems at room temperature for 2 days to ensure a homogeneous drying and to prevent twisting and bending. Finally, the sintering schedule had been carried out at different final temperatures to improve the porosity, the quality, and the mechanical properties of the support.

2.1.2.1. Sintering programs. The preparation of porous ceramic supports for membranes requires a programmable furnace at different final temperature. In accordance with this idea, we have used two temperature plates. In the first part, the sample was heated with a speed of 2 °C/min until 250 °C and was maintained for 120 min at this temperature of decomposition to remove organic additives such as methocel, amijel, and starch. Careful work is needed at the second part of sintering to avoid the formation of cracks in the samples. The firing temperature was fixed at 950, 1000, or 1100 °C for 3 h. The detailed program is explained in Fig. 6.

2.1.2.2. Visual characterization. The variation in sintering temperature changes the coloration of supports from yellowish to dark gray (see Fig. 7). This transformation of color is because of the oxidation of Fe. Table 4 tracks the

Table 2
Chemical analysis of fractions < 2 μm of smectite clay.

Chemical composition	SiO_2	Al_2O_3	Fe_2O_3	CaO	MgO	SO_3	K_2O	Na_2O	TiO_2	Cl^-
Raw clay, weight %	70.5	14.31	5.15	2.4	2.89	0.21	0.52	2.52	0.2	0.01

Table 3
XRD "*d*" values of clay fraction.

d (Å)	Possible minerals
3.34	Quartz
3.03	Calcite
12.62	Smectite
7.14	Kaolinite

Table 4
Variation in support diameter with different sintering temperatures.

Different sintering		
Temperature (°C)	External diameter	Internal diameter
950	3.7%	2%
1000	5%	4%
1100	8.75%	5.2%

size of external and internal diameter during the sintering process. After thermal treatment, the diameter of each support decreases, which is due to the presence of shrinkage phenomena.

2.2. Characterization methods

Clay was subjected to X-ray fluorescence (XRF) to analyze the chemical composition or elements present in the sample. XRF measurements were performed using a commercial instrument (ARL 9900 of Thermo Fisher) with monochromatic radiation K_{al} of cobalt ($\lambda = 1.788996$ Å). Phases present in the powder composition were analyzed by an X-ray diffractometer using Panalytical X'Pert High-score plus diffractometer with Cu Kα radiation ($\lambda = 1.5406$ Å).

The identification of functional groups present in clay was performed by the Fourier transform infrared (FTIR) spectroscopy. FTIR spectrum was collected using a Perkin Elmer 783 dispersive spectrometer in the range of 4000–400 cm^{-1}. The sample was prepared as KBr pellet.

A scanning electron microscopy (SEM) and transmission electron microscopy (TEM) were used to determine the sample morphology and the microstructure formed before and after sintering the materials.

The mechanical test was obtained using a machine EZ50 (50 kN). Samples were analyzed three times using tensile tests with NEXYGEN Plus software.

The differential thermal analysis (DTA) and thermogravimetric analysis (TGA) were carried out at temperature ranging between 0 and 1000 °C at a rate of 5 °C/min under nitrogen.

3. Results and discussion

3.1. Characterization of the raw clay

3.1.1. XRF characterization

It was necessary to know the chemical compositions of the minerals that are present in the clay. In XRF technique, fluorescent *X-rays are emitted from a material that has been excited by bombarding with high-energy X-rays*. The data given in Table 2 show that the clay was made up of silica, alumina, calcium, sodium, magnesium, and iron oxides in major quantities and other elements in trace amounts.

3.1.2. FTIR characterization

To investigate the surface characteristics of bentonite, vibrational spectra by means of FTIR spectroscopy have been investigated (Fig. 1). The fundamental stretching vibrations of different -OH groups present in Mg–OH–Al, Al–OH– Al, and Fe–OH–Al units in the octahedral layer were observed at 3412 cm^{-1} with a large band [22]. A broad

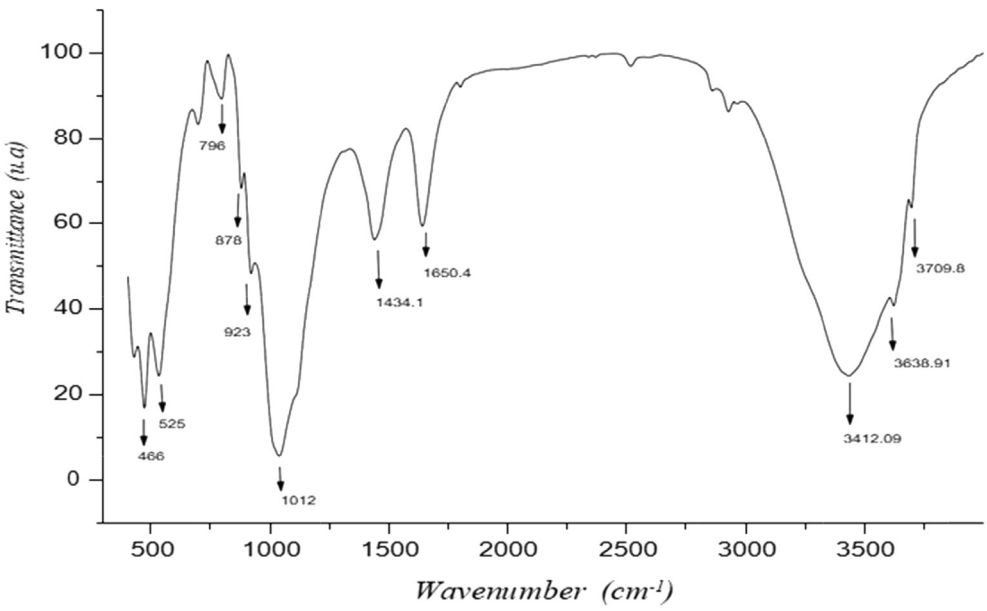

Fig. 1. Infrared spectra of raw smectite.

band at 3412 cm^{-1} corresponds to OH frequencies (silanol groups (Si–O–H)). The band that arises at 1650 cm^{-1} in the spectrum of clay suggests the presence of the characteristic band of the interlayer hydrogen. In case of bands corresponding to Al–Al–OH, bending vibrations are observed at 918 cm^{-1}. An intense peak appears at 3638 cm^{-1}, which indicates the possibility of the hydroxyl linkage [23,24]. The bending mode of Si–O is strongly evident in the silicate structure, showing absorption bands at 1012, 1111, 525, and 466 cm^{-1} arising from the stretching and bending vibrations of SiO_2^- tetrahedral [22–25]. A very strong band in the range of 1111–1012 cm^{-1} appeared to be similar to Si–O stretching vibrations of the tetrahedral layer. The peaks at 525 cm^{-1} and the weak band at 466 cm^{-1} are due to Mg–O–Si and Al–O–Si bending vibrations, respectively. Si–O stretching vibrations were observed at 796 cm^{-1}, which supports the presence of quartz. The presence of calcium combined with carbonate species reveals the existence of calcite as confirmed by FTIR at 1434 cm^{-1} and fluorescent X-ray.

3.1.3. X-ray diffraction characterization

Clay is composed mostly of silica, alumina, and water, frequently with appreciable quantities of iron, alkalis, and alkali earths [26]. X-ray diffraction (XRD) analysis was applied to understand and define the mineralogical composition of the raw clay (Fig. 2). The composition of clay was identified by comparing "*d*" values. Results indicate the presence of smectite, kaolinite, quartz, and calcite phases (Table 3) and the sodic character of this clay.

3.1.4. SEM analysis

SEM provides information related to morphology and texture of our materials. The SEM pictures (Fig. 3) with

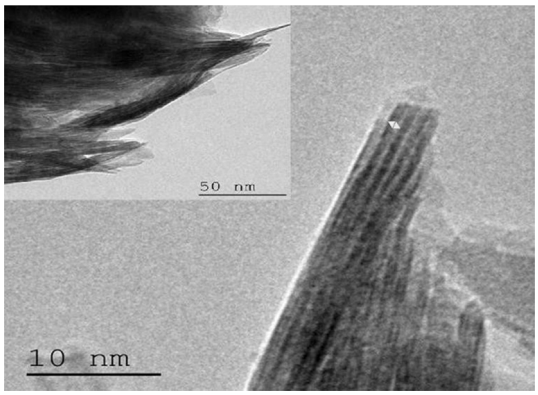

Fig. 3. SEM micrographs of raw smectite with different magnifications.

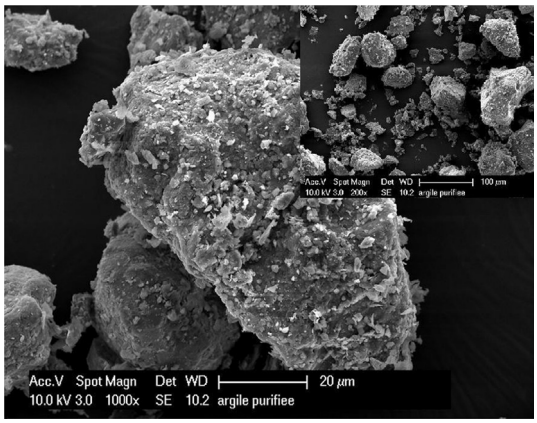

Fig. 4. TEM of raw smectite.

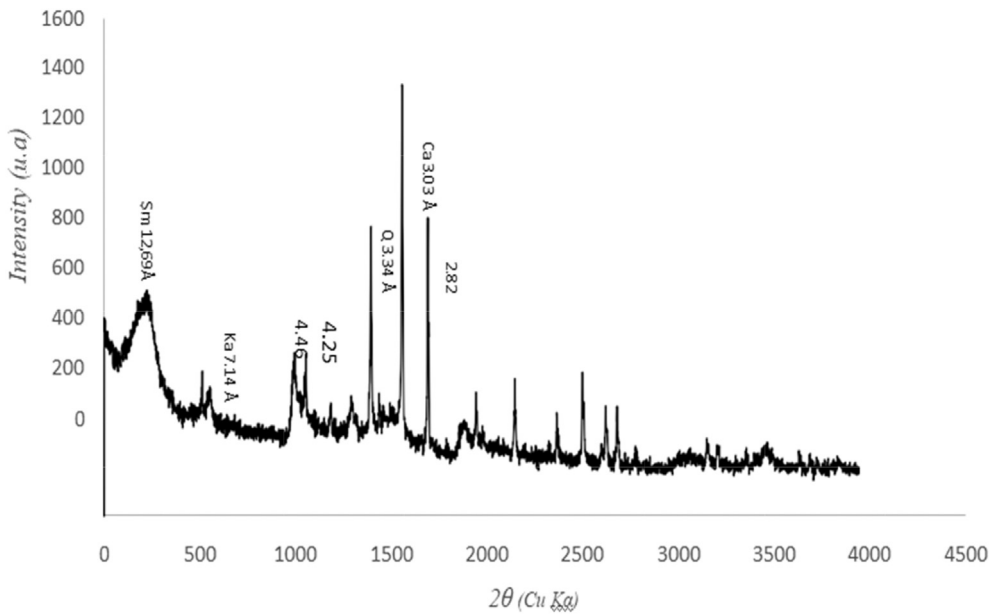

Fig. 2. XRD pattern of the pure smectite (Sm = smectite, Ka = kaolinite, Q = quartz, and Ca = calcite).

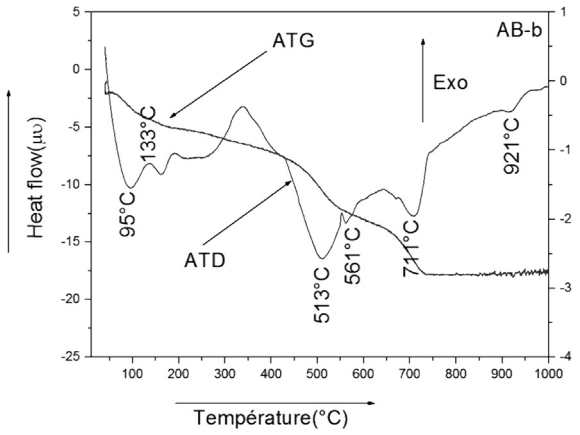

Fig. 5. DTA and TGA curves of smectite (AB-b).

different magnifications indicated the presence of diverse size of particles with a diameter of the range of 1.5 µm.

3.1.5. TEM analysis

TEM photomicrographs of raw clay show (Fig. 4) the distribution of platelets per stack.

3.1.6. Thermal analysis

DTA curves (Fig. 5) were acquired by heating raw clay from 27 to 1000 °C at a constant rate of approximately 5 °C. The bentonite shows two endothermic peaks: the first peak at 95 °C corresponding to the loss of water held between the basal planes of the lattice structure (swelling water) [27], and the second peak at 513 °C corresponding to the dehydroxylation of its minerals. These two endothermic peaks are followed by another peak, which takes place at 921 °C characteristic of aluminum ferifere [28]. An

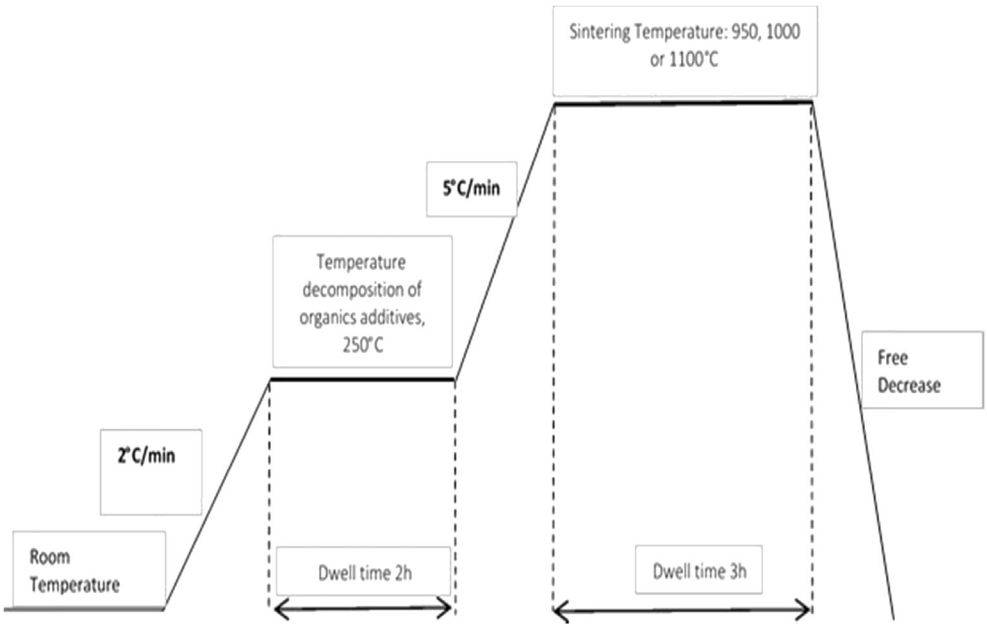

Fig. 6. The different sintering programs of temperature–time used in this study.

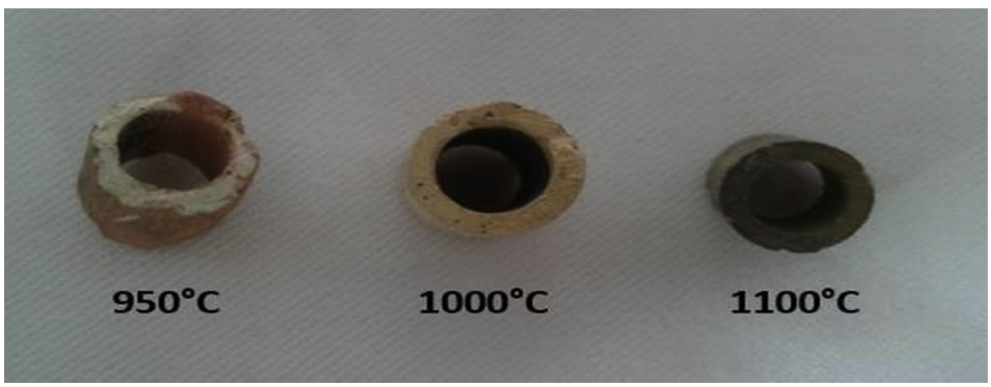

Fig. 7. Tubular support after sintering at different temperatures: 950, 1000, and 1100 °C.

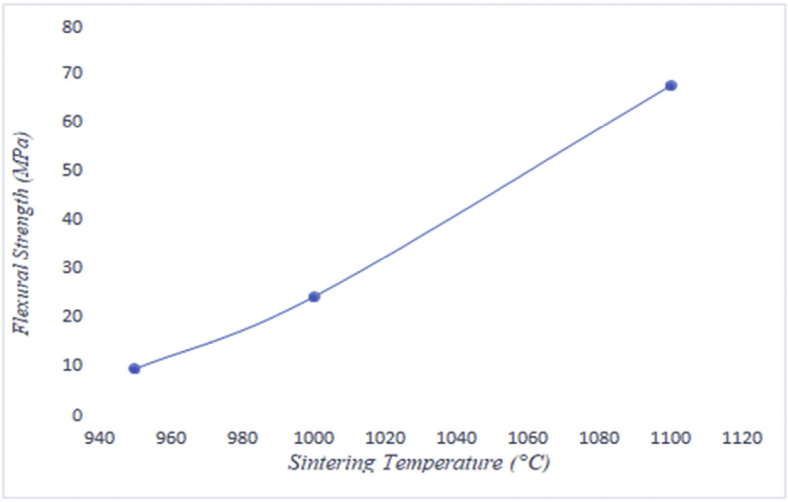

Fig. 8. Flexural strength of the sample versus sintering temperature.

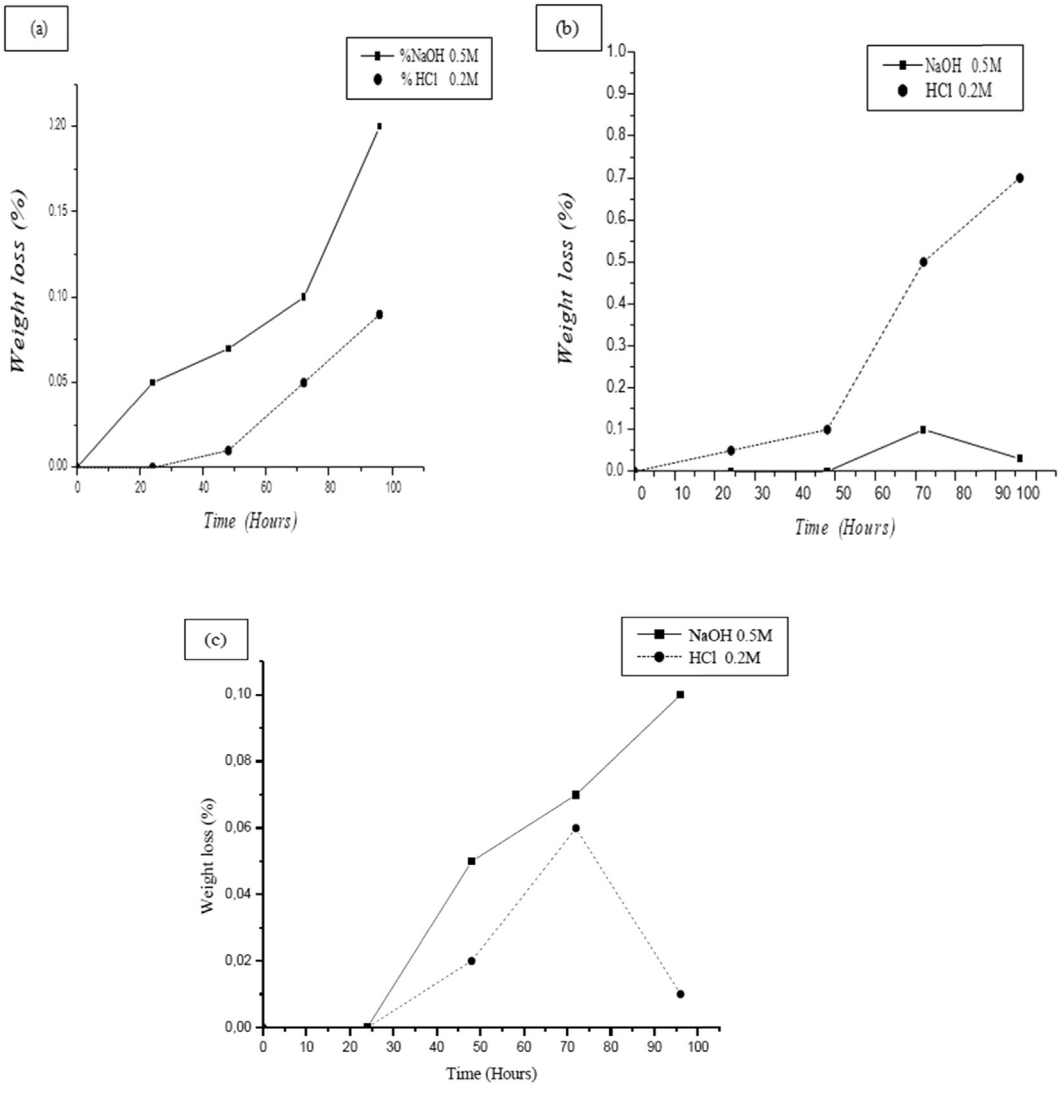

Fig. 9. Weight loss versus time of supports sintered at 950 (a), 1000 (b), and 1100 °C in acidic and basic solutions.

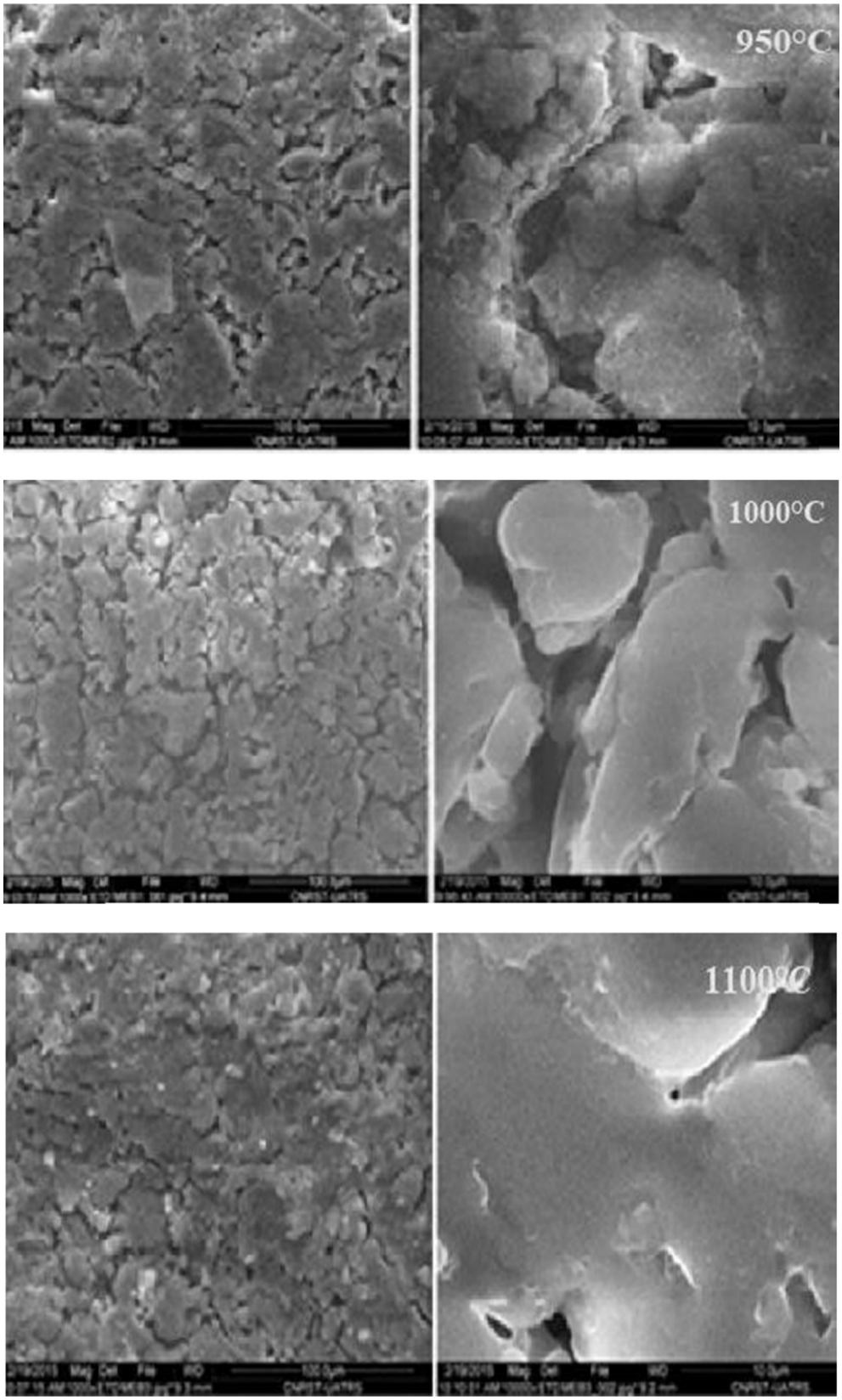

Fig. 10. SEM micrographs of a membrane sintered at different temperatures. Two magnifications, ×1000 and ×10.000 are shown.

endothermic reaction appears at 561 °C, which can be attributed to the transformation of quartz. Finally, the decomposition of carbonate occurred at 711 °C with a medium intensity.

The curves of TGA (Fig. 5) permit us to estimate the weight loss of sample. The curves present three mass losses: the first one is between 100 and 300 °C, because of the moisture and water interlayer. The second mass loss between 513 and 512 °C relates to the loss of water content. Finally, the third mass loss takes place at 561 °C, which corresponds to the decarbonization of clay.

3.2. Characterization of the support

For the development of high-quality supports, mechanical and chemical properties and hydraulic permeability are the most important variables.

3.2.1. Mechanical strength

The mechanical resistance test was carried out by using the three-point bending strength. The length, width, and thickness of the sample were 4.5, 1.5, and 3 mm, respectively. Results of mechanical properties (Fig. 8 and Table 4) confirm the hypothesis that the sintering temperature leads to a variation in flexural strength of the tubular support. An increase in the sintering temperature caused a rise in the mechanical strength. Densification phenomena occurred at 1100 °C, which provides 67.61 MPa as a flexural strength due to the growth of grain boundaries. These results are in good agreement with other supports with different materials [30–33].

3.2.2. Chemical resistance

Chemical resistance tests were carried out by the use of HCl (0.2 M) and NaOH (0.5 M) at the ambient temperature (27 °C). The results are reported in Fig. 9, giving an explanation to the variation in sintering temperature at 950, 1000, and 1100 °C with the acidic and basic solutions under the same conditions of time and temperature. The weight loss of a sample placed in soda and chloride acid solution for more than 96 h was insignificant. As a final point, no phenomena such as color change, degradation, or aging of sample were detected.

3.2.3. SEM analysis

SEM examined evolution of the densification phenomenon and changes in surface quality. Fig. 10 shows the internal surface of tubular supports heated at 950, 1000, and 1100 °C. These micrographs prove the absence of any cracks and reveal homogeneity of the surface. Furthermore, the sintering process causes an increase in the pore diameter. This is because of the generation of a vitreous mass by fused silica and some impurities present in the clay. The phenomenon of fusion was seen clearly beyond 1100 °C. The values of pore size estimated from SEM images are 0.8, 1.7, and 2.3 μm for 950, 1000, and 1100 °C, respectively.

3.2.4. Water permeability

To evaluate the performance and the presence of defects in the ceramic supports, water flux characterization was used with transmembrane pressure between 0 and 3 bar. The permeability of the support was determined using the variation in distilled water flux J_w (L h^{-1} m^{-2}) with transmembrane pressure (bar) according to the Darcy law (Eq. 1)):

$$J_w = L_p \times \Delta P \quad (1)$$

Sintering temperature and mechanical resistance are the key parameters to make decision about the optimal temperature. The formation of grain boundaries begins at 950 °C; however, a low mechanical strength (see Table 5) has been noted at this temperature. At 1100 °C the phenomenon of fusion starts (see Fig. 11) because of the formation of vitreous mass by fused silica and some impurities present in the clay. Eventually the best conditions are established to 1000 °C, with an average pore diameter 1.7 μm and 24.06 MPa as a flexural strength.

The tubular support was immersed in pure distilled water for a minimum of 24 h before filtration tests at room temperature. The experiments show that the increase in the pressure causes a linear increase in the water flux. The support permeability (L_p) was equal to 525 L h^{-1} m^{-2} bar^{-1}.

Smectite in tubular configuration with a mean pore size 1.7 μm, 24.06 MPa as a flexural strength, and permeability 525 L h^{-1} m^{-2} bar^{-1} seems to be favored compared with different results summarized in Table 6 from 2009 until 2018. It is interesting to mention that the mixing of methocel, amijel, starch, and water with different amounts proved to be effective.

The development of ceramic membrane supports based only on natural materials using the most abundant and cheaper additives in nature was investigated to attend the economic advantages.

Table 5
Mechanical resistance results of different sintering temperature.

Sintering temperature (°C)	950 °C	1000 °C	1100 °C
Force (N)	10.93	25.81	72.89
Elongation (mm)	0.11	0.15	0.17
Flexural strength (MPa)	9.28	24.06	67.61

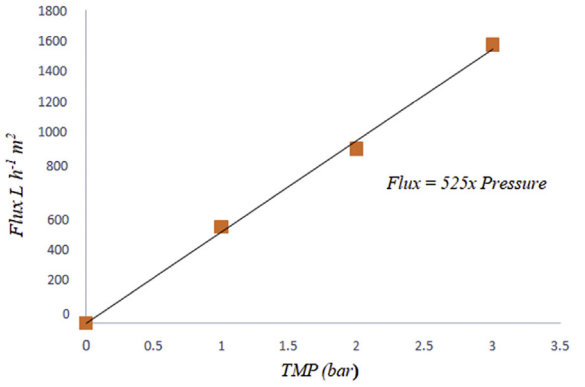

Fig. 11. Water flux permeability versus pressure of support sintered at 1000 °C.

Table 6
Summary of different ceramic membrane support.

References, years	Materials		Sintering temperature (°C)	Mean pore size (μm)	Water permeability (L h^{-1} m^{-2} bar^{-1})	Mechanical strength (MPa)	Applications
[34], 2012	Perlite with organic additives: methocel (as a plasticizer), amijel (as a binder), starch (as a porosity agent), PEG (as a binder)	Macroporous support of perlite	1000	6.6	_	_	Wastewater treatment (effluent)
	Two layers of perlite with different granulomeres	Thin layer of perlite	930	0.27	815		
	Plane support						
[35], 2010	Smectite, kaolin, cornstarch, STTP Tubular configuration		1000	1.04	360–430	19	Filtration of bovine serum albumin Intercalation of support toward proteins issued from milk
[36], 2011	Perlite used in this study from Morocco Organic additives: methocel, amijel, starch, and PEG Flat membrane		1000	6.64	1797	_	Used to clarify a suspension of baking powder
[37], 2012	Clay with calcium carbonate tubular configuration Organic additives: amijel, methocel, and starch		1250	3.4	–	–	Effluent treatment
	Thin layer with zirconia Support		1050	2.5	1000		
[38], 2013	Kaolin with calcium carbonate Tubular configuration		1150	1.3	12,244	25	Effluent treatment
[39], 2017	Bentonite The powder used with micronized phosphate (30 wt %)		950	1.8	725	14.6	The use of a thin layer with TiO_2 improved the permeability of the membrane (33) with mean pore diameter, 72 nm This membrane was applied for dye removal
[40], 2018	Natural perlite (5 wt %) starch as porosity agent Flat membrane		950	1.7	1433.46	21.68	Effluent treatment (agro-food and tannery)
This work, 2018	Natural bentonite from Tunisia Organic additives: amijel, methocel, and starch Tubular configuration		1000	1.7	525	24	–
[41], 2009	Support		700	4.5	_	_	Dying effluent (textile industry)
	Active layer		800	0.25	475		

STTP: sodium tripolyphosphate; PEG: polyethylene glycol.

4. Conclusion

In this study, a low-cost support made of Tunisian clay was developed. The support was prepared by extrusion of the clay paste and sintering at different temperature for 3 h. The mechanical and chemical properties of the support are satisfying in terms of pore diameter. The elaboration of ceramic support has exhibited higher water permeability, equal to 525 L h^{-1} m^{-2} bar^{-1}. These supports should find application for economic treatment of wastewater containing bacteria and/or microbes in emergent countries.

Acknowledgments

The authors gratefully acknowledge Professor Ezzeddine SRASRA, Centre National de Recherches Scientifiques des Matériaux Technopôle de Borj Cedria, Tunisia, and Professor Raja BEN AMAR, Laboratoire des matériaux et environnement, Faculté des Sciences de sfax, Université de Sfax, Tunisia, for providing instrumental and laboratory facilities.

References

[1] Coping with water scarcity: Challenge of the Twenty-first Century, U.N. water, Food and Agricultural Association, 2007.
[2] K. Scott, Microfiltration, Handbook of Industrial Membranes, Elsevier Sci., Oxford, UK, 1995, pp. 373–429.
[3] J. Benito, M. Sanchez, P. Pena, M. Rodriguez, Desalination 214 (2007) 91–101.
[4] M. Ulbright, Polymer 47 (2006) 2217–2262.
[5] P. Bernardo, E. Drioli, G. Golemme, Ind. Eng. Chem. Res. 48 (2009) 4638–4663.
[6] M.K. Uddin, Chem. Eng. J. 308 (2017) 438–462, https://doi.org/10.1016/j.cej. 2016.09.029.

[7] F. Bouzerara, A. Harabi, S. Achour, A. Larbot, J. Eur. Ceram. Soc. 26 (2006) 1663–1671.
[8] M. Mamoudi, A. Larbot, H.E. Feki, R.B. Amar, Ceram. Int. 33 (2007) 337–344.
[9] N. Saffaj, S. Alami-Younssi, A. Albizane, A. Messouadi, M. Bouhria, M. Persin, M. Cretin, A. Larbot, Separ. Purif. Technol. 36 (2004) 107–114.
[10] N. Saffaj, M. Persin, S. Alami-Younssi, A. Albizane, M. Bouhria, H. Loukili, H. Dach, A. Larbot, Separ. Purif. Technol. 47 (2005) 36–42.
[11] N. Saffaj, M. Persin, S. Alami-Younssi, A. Albizane, M. Cretin, A. Larbot, Appl. Clay Sci. 31 (2006) 110–119.
[12] B. Archiou, H. Elomari, M. Ouammou, A. Albizane, J. Bennazha, S. Alami-Younssi, I.E. El Amrani, A. Aaddane, J. Mater. Environ. Sci. 7 (1) (2016) 196–204.
[13] J. Fang, G. Qin, W. Wei, X. Zhao, L. Jiang, Desalination 311 (2013) 113–126.
[14] I. Barrouk, S. Alami Younssi, A. Kabbabi, M. Persin, A. Albizane, S. Tahiri, J. Mater. Environ. Sci. 6 (8) (2015) 2190–2197.
[15] M. Sayehi, R. Dhouib Sahnoun, S. Fakhfekh, S. Baklouti, Ceram. Int. 44 (5) (2018) 5202–5208.
[16] F. Ayari, E. Srasra, M. Trabelsi-Ayadi, Desalination 185 (2005) 391–397.
[17] A. Talidi, N. Saffaj, K.E. Kacemi, S.A. Younssi, A. Albizane, A. Chakir, Sci. Study Res. Chem. Chem. Eng. Biotechnol. Food Indus. 12 (2011) 263–268.
[18] E. Jung-Hye, K. Young-Wook, S. In-Hyunck, J. Korean Ceram. Soc. 50 (5) (2013) 341–347.
[19] R. Vioth Kumar, A.K. Ghoshal, G. Pugazhenthi, J. Membr. Sci. 490 (2015) 92–102.
[20] Y. Dong, X. Feng, D. Dong, S. Wang, J. Yang, J. Gao, X. Lin, G. Meng, J. Membr. Sci. 304 (1–2) (2007) 65–75.
[21] P. Hristov, A. Yoleva, S. Djambazov, I. Chkovska, D. Dimitrov, J. Univ. Chem. Technol. Metall. 47 (7) (2012) 476–480.
[22] V.C. Farmer, in: V.C. Farmer (Ed.), The Infrared Spectra of Minerals, Mineralo. Soc., 1974, pp. 331–363.
[23] J. Madejova, P. Komadel, B. Cicel, Ser. Clays 1 (1992) 9–12.
[24] E. Srasra, F. Bergaya, J.J. Fripiat, Clays Clay Miner. 42 (3) (1994) 237–241.
[25] S. Hayakawa, L.L. Hench, J. Non-Cryst. Solids 262 (2000) 264–270.
[26] R.E. Grim, 1968 Clay Mineralogy, McGraw Hill Book Co, New York, 1902.
[27] S.B. Hendricks, R.A. Nelson, L.T. Alexander, J. Am. Chem. Soc. 62 (1940) 1457–1464.
[28] R.E. Grin, G. Kulbicki, Am. Min. 46 (1961) 1329–1333.
[29] D. Vasanth, G. Pugazhenthi, R. Uppaluri, J. Membr. Sci. 379 (2011) 154–163.
[30] S. Khemekhem, R. Ben Amar, R. Ben Hassen, A. Larbot, A. Ben Salah, L. Cot, Eur. J. Control 31/2 (2006) 165–181.
[31] P. Monash, G. Pugazhenthi, Appl. Ceram. Technol. 8 (1) (2011) 227–238.
[32] I. Hedfi, N. Hamdi, E. Srasra, H.A. Rodriguez, Appl. Clay Sci. 101 (2014) 574–578.
[33] L. Young- II, E. Jung-Hye, K. Young-Wook, S. In-Hyunck, J. Korean Ceram. Soc. 51 (5) (2014) 380–385.
[34] A. Majouli, S. Tahiri, S. Alami Younssi, H. Louhili, A. Albizane, Ceram. Inter. 38 (2012) 4294–4303.
[35] S. Fakhfekh, S. Baklouti, S. Baklouti, J. Bouaziz, Adv. Appl. Ceram. 109 (1) (2010) 31–38.
[36] A. Majouli, S. Alami Younssi, S. Tahiri, A. Albizane, H. Loukili, M. Belhaj, Desalination 277 (1–3) (2011) 61–66.
[37] F. Bouzerara, A. Harabi, B. Ghouli, N. Medjemem, B. Boudaira, S. Condom, Procedia Eng. 33 (2012) 278–284.
[38] B. Ghouil, A. Harabi, F. Bouzerara, N. Briki, Desalin. Water Treat. (1–5) (2013) 16–17.
[39] A. Bouazizi, M. Breida, A. Karim, B. Achiou, M. Ouammou, J.I. Calvao, A. Aaddane, K. Khiat, S. Alami Younssi, Ceram. Int. 43 (1) (2017) 1479–1487.
[40] S. Saja, A. Bouazizi, B. Achiou, M. Ouammou, A. Albizane, J. Benraza, S. Alami Younssi, J. Environ. Chem. Eng. 6 (1) (2018) 451–458.
[41] I. Jedidi, S. Saida, S. Khemekhem, A. Larbot, N. Elloumi-Ammar, A. Fourati, A. Charfi, A. Ben Salah, A. Ben Amar, J. Hazard Mater. 172 (1) (2009) 152–158.